Natural History and Disease Progression of Early Cardiac Amyloidosis Evaluated by Echocardiography

Osnat Itzhaki Ben Zadok, MD, MSc[a,b,*], Alon Eisen, MD[a,b], Yaron Shapira, MD[a,b], Daniel Monakier, MD[a,b], Zaza Iakobishvili, MD, PhD[b,c], Shmuel Schwartzenberg, MD[a,b], Aryeh Abelow, MD[a,b], Hadass Ofek, MD[a,b], Shirit Kazum, MD[a,b], Binyamin Ben-Avraham, MD[a,b], Ashraf Hamdan, MD[a,b], Tamir Bental, MD[a,b], Alik Sagie, MD[a,b], Ran Kornowski, MD[a,b], and Mordehay Vaturi, MD[a,b]

Since the diagnosis of cardiac amyloidosis (CA) is often delayed, echocardiographic findings are frequently indicative of advanced cardiomyopathy. We aimed to describe early echocardiographic features in patients subsequently diagnosed with CA. Preamyloid diagnosis echocardiographic studies were screened for structural and functional parameters and stratified according to the pathogenetic subtype (immunoglobulin light-chain [AL] or amyloid transthyretin [ATTR]). Abnormalities were defined based on published guidelines. Our cohort included 75 CA patients of whom 42 (56%) were diagnosed with AL and 33 (44%) with ATTR. Forty-two patients had an earlier echocardiography exam available for review. Patients presented with increased wall thickness (1.3 [interquartile range {IQR} 1.0, 1.5] cm) ≥3 years before the diagnosis of CA and relative wall thickness was increased (0.47 [IQR 0.41, 0.50]) ≥7 years prediagnosis. One to 3 years before CA diagnosis restrictive left ventricular (LV) filling pattern was present in 19% of patients and LV ejection fraction ≤50% was present in 21% of patients. Right ventricular dysfunction was detected concomitantly with disease diagnosis. The echocardiographic phenotype of ATTR versus AL-CA showed increased relative wall thickness (0.74 [IQR 0.62, 0.92] versus 0.62 [IQR 0.54, 0.76], p = 0.004) and LV mass index (144 [IQR 129, 191] versus 115 [IQR 105, 146] g/m^2, p = 0.020) and reduced LV ejection fraction (50 [IQR 44, 58] versus (60 [IQR 53, 60]%, p = 0.009) throughout the time course of CA progression, albeit survival time was similar. In conclusion, increased wall thickness and diastolic dysfunction in CA develop over a time course of several years and can be diagnosed in their earlier stages by standard echocardiography. **(Am J Cardiol 2020;133:126−133)**

Cardiac amyloidosis (CA) is caused in the majority of cases by the cardiac infiltration of either immunoglobulin light chain (AL) or amyloid transthyretin (ATTR), and carries a poor prognosis.[1] Echocardiography is a useful tool for the assessment of cardiac amyloid burden through quantification of left ventricular (LV) size, mass, and wall thickness as well as LV diastolic function.[2] Since the clinical diagnosis of CA is often delayed, its typical echocardiographic phenotype consists of severe wall thickening and restrictive diastolic dysfunction.[2-4] In contrary, there are limited published data describing the echocardiographic characteristics of early CA and the natural course of disease progression.[3,5,6] Recently, we reported a mild increase in LV wall thickness concomitantly with the diagnosis of carpal tunnel syndrome and preceding the diagnosis of amyloidosis.[7] In this study, we sought to characterize sequential early echocardiographic features in patients subsequently diagnosed with CA and to delineate disease progression as assessed by echocardiography.

Methods

The population of the current study was comprised of consecutive AL and ATTR CA patients treated at our institution (Rabin Medical Center, Israel) between the years 2003 and 2019. For all patients, electronic medical records and echocardiographic examinations were retrospectively reviewed.

The diagnosis of AL was made in the presence of a monoclonal protein (identified by serum and urine protein immunofixation plus serum-free light chain assay) and histological evidence of amyloid deposition in tissue biopsy by Congo red staining. Further protein analysis confirming light chain deposits was made by immunohistochemistry.[8] Mass spectrometry proteomic analysis was undertaken in selected cases. The detection of cardiac amyloid involvement in AL was based on either cardiac magnetic resonance (CMR) imaging or endomyocardial biopsy (EMB). Patients who were deferred by their treating physician from CMR or EMB (high-risk patients) were provisionally diagnosed on the basis of typical echocardiographic features (concentric

[a]Department of Cardiology, Rabin Medical Center, Petah Tikva, Israel; [b]Sackler Faculty of Medicine, Tel Aviv University, Tel Aviv, Israel; and [c]"Clalit" Health Services, Tel-Aviv, Israel. Manuscript received June 17, 2020; revised manuscript received and accepted July 20, 2020.

Funding: none.

See page 132 for disclosure information.

*Corresponding author: Tel: 972-3-9377111; fax: 972-3-9213221.

E-mail address: osnat.itzhaki@gmail.com (O. Itzhaki Ben Zadok).

0002-9149/
https://doi.org/10.1016/j.amjcard.2020.07.050

LV thickening and diastolic dysfunction), as previously reported.[2] The diagnosis of ATTR was established based on either (1) EMB with confirmed amyloid deposits through Congo red staining with further subtyping, or, (2) technetium pyrophosphate nuclear scintigraphy (99mTc-PYP) with myocardial tracer uptake analysis using the semiquantitative visual score (≥2) and the quantitative heart to contralateral ratio ≥1.5.[9,10] The exclusion of light chain monoclonality by serum-free light chain and serum and urine immunofixation was mandatory in all patients diagnosed with ATTR.[10] Following a histological or noninvasive diagnosis of ATTR, all patients underwent TTR genetic testing to differentiate between mutant ATTR and wild-type ATTR.

We analyzed the resting echocardiographic parameters of patients with CA by screening the electronic database for examinations performed at and before the diagnosis and treatment of amyloidosis according to prespecified retrospective time points: (1) <1 year prediagnosis, (2) 1≤ year <3 prediagnosis, and (3) ≥3 years prediagnosis. The left atrial and ventricular diameters and LV ejection fraction (LVEF) were measured according to accepted guidelines.[11] Relative wall thickness (RWT) was calculated as 2 times LV posterior wall (PW) diastolic thickness divided by LV diastolic diameter.[11] LV mass was calculated according to the Devereux formula[12]: 1.04 (LV diastolic diameter + interventricular septal diameter + LV PW diastolic thickness)^3 − (LV diastolic diameter^3) − 13.6. Right ventricular (RV) function was evaluated qualitatively by visual assessment.[13] The pulmonary artery systolic pressure was estimated from peak velocity of the tricuspid regurgitation jet and estimated right atrial pressure based on inferior vena cava diameter and distensibility.[13]

LV diastolic function was assessed by recording mitral flow with standard pulsed Doppler technique, and measurements of early diastolic peak flow velocity (E), late diastolic peak flow velocity (A) and the ratio of early to late flow velocity peaks (E/A ratio).[14] We graded LV diastolic function in the absence of more than mild mitral regurgitation as follows: Grade 1 (impaired relaxation pattern), E/A ratio <0.8; Grade 2 (pseudonormal pattern), E/A ratios between 0.8 and 2; Grade 3 (restrictive pattern), E/A ratio >2.[14,15]

Cut-off values for defining abnormalities in the reported echocardiographic variables were chosen according to published reference guidelines in the general population.[11,15-18] Significantly increased wall thickness was defined as ≥1.4 cm of either interventricular septal or PW. Significant diastolic dysfunction was defined as either pseudonormal or restrictive LV diastolic patterns (Grade 2 and Grade 3). LV systolic dysfunction was defined as LVEF ≤50% and RV systolic dysfunction was defined by visual estimate.

Patients were excluded if the diagnosis of CA did not meet the above criteria. For the preamyloid diagnosis echocardiographic analysis we carefully reviewed the electronic medical records and echocardiography referral indications of study patients and excluded patients with clinically suspected amyloidosis at the time when the echocardiography exam was performed (Supplementary Table 1).

Mortality during follow-up was determined for all patients through the Israeli National Population Registry. The study protocol was approved by our Institutional Review Board.

The statistical analysis for this study was generated using SAS Software, Version 9.4 (SAS Institute Inc., Cary, NC). Continuous variables were presented by median and interquartile 25th, 75th range. Categorical variables were presented by (N, %). *t* Test was used to compare the value of continuous variables, displaying normal distribution between study groups and the Wilcoxon test was used for non-Gaussian distributions. Chi-square (for more than 2 categorical values) or Fisher's exact test (for 2 categorical values) were used to compare the value of categorical variables between study groups. The cumulative incidence of death during study follow-up was assessed by Kaplan-Meier survival analysis, with the log-rank test. Two-sided p values less than 0.05 were considered statistically significant.

Results

Our study cohort included 75 patients with a diagnosis of CA of whom 42 (56%) and 33 (44%) had AL and ATTR, respectively. CA was either the leading clinical diagnosis or was diagnosed on imaging studies during an initial evaluation for systemic amyloidosis. Patients' baseline characteristics are presented in Table 1. The median age for the diagnosis of amyloidosis was 71 (25th, 75th interquartile

Table 1
Characteristics of patients with cardiac amyloidosis at diagnosis

Variable	Cardiac amyloidosis patients (n = 75)
Age at amyloidosis diagnosis (years)	71 (64, 80)
Women	23 (31%)
Diabetes mellitus	9 (12%)
Hypothyroidism	4 (5%)
Hypertension	23 (31%)
Coronary artery disease	9 (12%)
Atrial fibrillation	20 (27%)
Chronic kidney disease	10 (13%)
Moderate or severe aortic stenosis	0 (0%)
Carpal tunnel syndrome	32 (43%)
Immunoglobulin light-chain cardiac amyloidosis (n = 42)	
Typing by mass spectrometry	4 (10%)
Amyloid involvement	
Kidney	12 (29%)
Gastrointestinal and liver	8 (19%)
Soft tissue	2 (5%)
Fat pad*	4 (27%)
Bone marrow	12 (29%)
Evaluation for cardiac amyloidosis	
Cardiac magnetic resonance imaging	30 (71%)
Endomyocardial biopsy	8 (19%)
Echocardiography-based diagnosis	7 (17%)
Transthyretin cardiac amyloidosis (n = 33)	
Hereditary (mutant)	5 (15%)
Evaluation for cardiac amyloidosis	
Technecium-99m pyrophosphate scan	26 (79%)
Cardiac magnetic resonance imaging	24 (72%)
Endomyocardial biopsy	4 (12%)
Echocardiography-based diagnosis	1 (3%)

Data are presented as medians (25th, 75th quartiles) or as percentages, as appropriate.

* Fat-pad biopsies were performed in only 15 (36%) of patients with immunoglobulin light-chain amyloidosis.

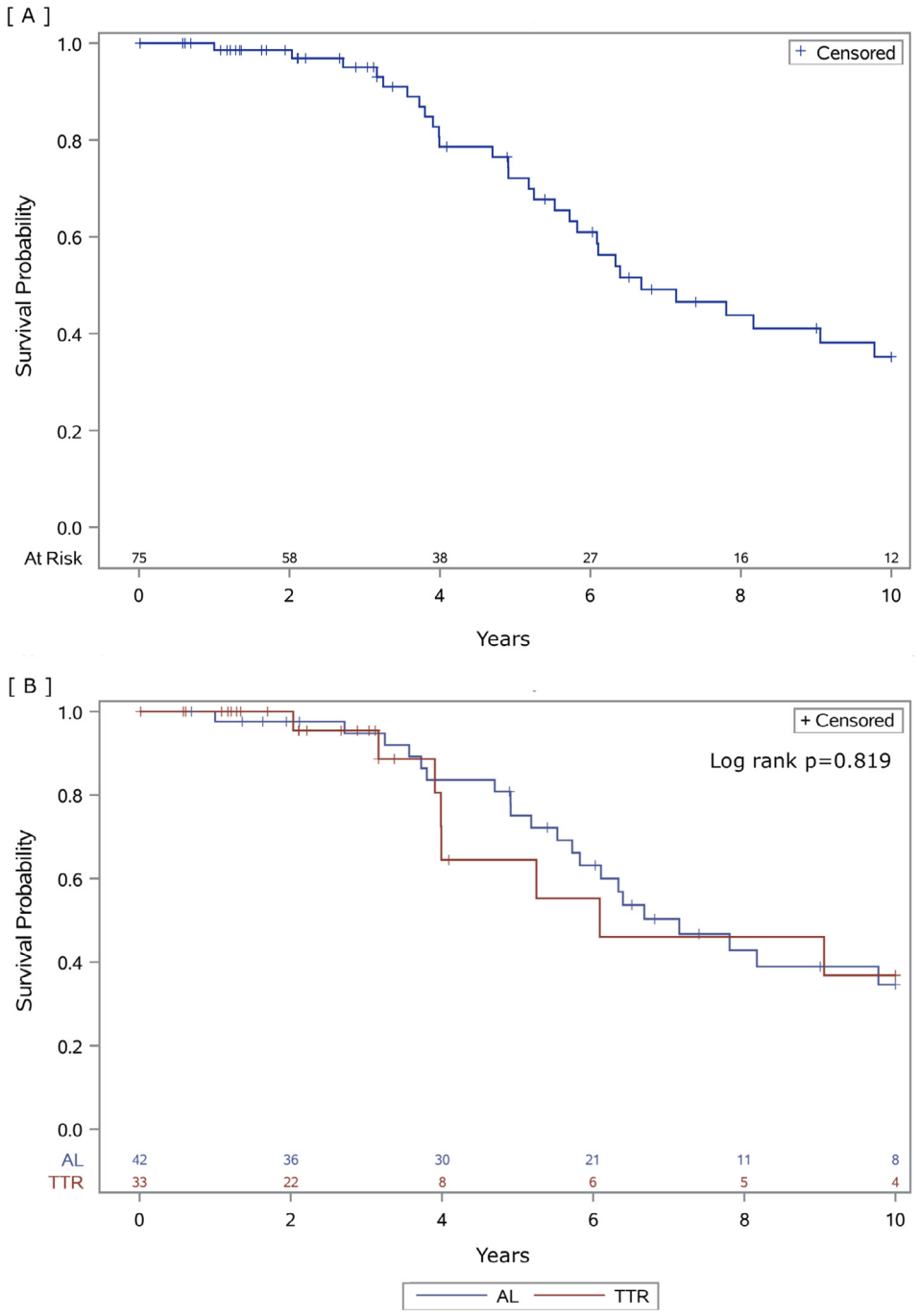

Figure 1. Kaplan-Meier curve of 10-year survival of patients with (*A*) CA, (*B*) CA stratified by its pathogenetic amyloid subtype. AL = immunoglobulin light-chain; ATTR = amyloid-transthyretin; CA = cardiac amyloidosis.

range [IQR] 64, 80) years with male predominance (69%). Amyloid cardiac involvement was established by CMR in the majority of AL and ATTR patients (72%). Approximately a third (27%) of the study population had atrial fibrillation and the rate of carpal tunnel syndrome was 43%. As shown in Figure 1 overall survival was 6.7 years.

The echocardiographic parameters of CA patients (n = 75) found within 1 year of diagnosis (<1 year prediagnosis) are presented in Table 2. Wall thickness and LV mass index were increased to 1.5 (IQR 1.3, 1.7) cm and 138 (IQR 114, 159) g/m^2, respectively. Significant diastolic dysfunction was present as determined by trans-mitral Doppler E/A ratio (91% of patients with Grade 2 or Grade 3 diastolic function) and an abnormal elevation in E/e' ratio (19 [IQR 14, 22]) by tissue Doppler (Figure 2). Approximately a third of patients presented with LV (37%) or RV (35%) systolic dysfunction.

We then stratified the echocardiographic parameters observed at the diagnosis of CA according to its pathogenetic subtype (Table 3). Patients with ATTR versus AL CA

Table 2
Echocardiographic findings and troponin levels in patients with cardiac amyloidosis at different time intervals before the diagnosis of amyloidosis

Variable	<1 year prediagnosis (n = 75)	1≤ year <3 prediagnosis (n = 33)	≥ 3 years prediagnosis (n = 24)
Median time prediagnosis (months)	5 (2, 0)	20 (12, 31)	60 (42, 76)
Left ventricular ejection fraction (median)	55 (47, 60)	60 (50, 60)	60 (60, 60)
Left ventricular ejection fraction ≤ 50%	28 (37%)	7 (21%)	3 (13%)
Right ventricular dysfunction	24 (35%)	1 (5%)	0 (0%)
Tricuspid annular plane systolic excursion	15 (13, 17)	Non-available	Non-available
Posterior wall (cm)	1.4 (1.3, 1.6)	1.3 (1.1,1.4)	1.2 (1.0, 1.4)
Ventricular septum (cm)	1.5 (1.3, 1.7)	1.4 (1.2, 1.6)	1.3 (1.0, 1.5)
Wall thickness ≥ 1.4 cm	60 (80%)	18 (55%)	8 (33%)
Left ventricular end diastolic diameter (cm)	4.2 (3.9,4.5)	4.6 (4.3, 4.8)	4.4 (4.2, 4.9)
Left ventricular end systolic diameter (cm)	2.8 (2.5, 3.4)	2.8 (2.7, 3.2)	2.8 (2.4, 2.9)
Relative wall thickness	0.67 (0.59, 0.79)	0.55 (0.38, 0.67)	0.50 (0.45, 0.58)
Relative wall thickness ≥ 0.42	73 (97%)	31 (94%)	24 (100%)
Left atrial area (cm^2)	24 (21, 28)	22 (19, 28)	21 (18, 26)
Left atrial diameter (cm)	4.3 (3.7, 4.7)	4.0 (3.9, 4.7)	4.0 (3.8, 4.4)
Left ventricular mass index (g/m^2)	138 (114, 159)	110 (94, 131)	Non-available
E/A	2.1 (1.6, 2.9)	2 (1.2, 2.9)	Non-available
Deceleration time (ms)	150 (117, 193)	Non-available	Non-available
e' lateral	4 (2.4, 5)	5 (4, 7)	Non-available
E/e'	19 (14, 22)	18 (16, 20)	Non-available
Systolic pulmonary artery pressure (mm Hg)	40 (30, 50)	42 (35, 58)	33 (31, 42)
Troponin^ (ng/L)	70 (49, 114)	35 (15, 77)	Non-available

Data are presented as medians (25th, 75th quartiles) or as percentages, as appropriate.
^ Troponin normal laboratory range <13 ng/L. Troponin levels 1≤ year <3 prediagnosis were available in 13 of 33 of patients.

had increased wall thickness, increased LV mass index, increased LA diameter and worse LV systolic function. LV diastolic function was similar between the 2 subgroups. Troponin level and survival rate of patients with AL-CA and ATTR-CA were similar (Figure 1).

To describe the natural progression of cardiac amyloid involvement we reviewed the echocardiographic parameters observed at prespecified time points before disease diagnosis (Table 2). Forty-two (56%) of study patients had an earlier echocardiography exam (≥ 1 year before the diagnosis of CA) available for review. The majority of patients (19 of 24, 79%) presented with increased wall thickness (≥ 12 mm 15) ≥ 3 years before the diagnosis of amyloidosis. Moderately increased (≥ 14 mm 11) wall thickness was documented 1≤ year <3 before CA diagnosis in 55% (18 of 33) of patients. The RWT was abnormal (>0.42[11,16]) in 64% (7 of 11) of patients ≥ 7 years before disease diagnosis (Supplementary Table 1). Significant LV diastolic dysfunction was present on echocardiography 1≤ year <3 before CA diagnosis with pseudonormal LV filling pattern (Grade 2) in 42% and restrictive LV filling pattern (Grade 3) in 19% of the cohort (Figure 2). LV systolic dysfunction was observed in 21% of the cohort 1≤ year <3 before the diagnosis of amyloidosis, whereas RV dysfunction was present only with disease diagnosis in 35% (n = 24).

Notably, troponin levels were elevated (~ 3*upper normal limit) 1≤ year <3 years before the diagnosis of amyloidosis (Table 2).

We subanalyzed the echocardiographic parameters observed before the diagnosis of amyloidosis according to its pathogenetic subtype (Table 3). We found increased wall thickness and RWT in patients with ATTR versus AL 1≤ year <3 preamyloid diagnosis. Moreover, worse diastolic function was demonstrated 1≤ year <3 prediagnosis in patients with ATTR versus AL (79% vs 14% of patients with Grade 2 and Grade 3 diastolic patterns).

To evaluate the time frame for the development of cardiac amyloid involvement, we performed a separate analysis which included only patients who underwent at least 2 echocardiographic examinations during the study follow-up period with the earlier exam demonstrating normal-range values for the investigated parameter (Figure 3). We found that the maximal time frame as assessed by echocardiography for the development of wall thickness ≥ 1.4cm was at a median of 2.3 years from the documentation of normal-range values (n = 23), and that the maximal time frame for the development of Grade 2 or Grade 3 diastolic dysfunction was at a median of 2.9 years from the documentation of either normal or Grade 1 diastolic pattern (n = 18). LV and RV systolic dysfunction were noted at median time frames of 2.6 and 2.3 years from the documentation of normal-range values, respectively (n = 14).

We also investigated the time interval from the echocardiographic documentation of significant structural and functional abnormalities to disease diagnosis (Figure 3). Wall thickness ≥ 1.4 cm and Grade 2 or Grade 3 LV diastolic dysfunction were observed approximately a year before disease diagnosis.

Discussion

This study provides new insights into the understanding of the natural progression of CA by retrospectively evaluating echocardiographic parameters before its clinical diagnosis. We found that: (1) Wall thickening and diastolic dysfunction develop over a course of 2 to 3 years and precede the functional deterioration of the ventricles by several years (Figure 4); (2) Echocardiographic features along the

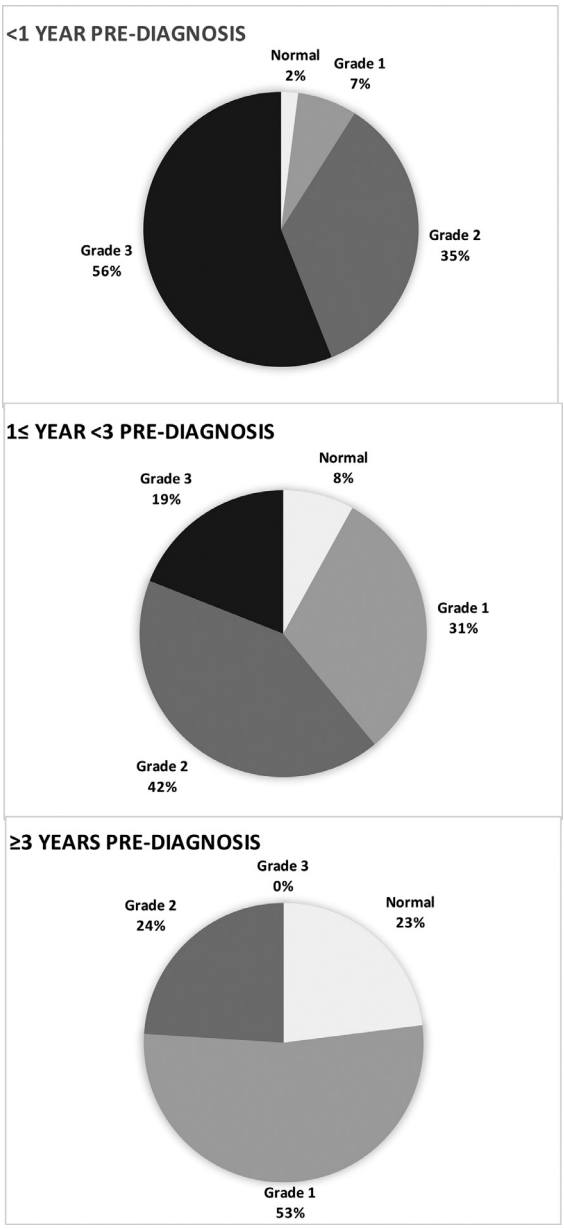

Figure 2. LV diastolic function in patients with CA at different time points before the diagnosis of amyloidosis. CA = cardiac amyloidosis; LV = left ventricular.

time course of CA progression demonstrate advanced cardiomyopathy in patients with ATTR versus AL; (3) Significant wall thickening and diastolic dysfunction are present approximately a year before the diagnosis of CA.

CA is an increasingly recognized diagnosis due to improved and novel diagnostic modalities[2, 10] and to the development of new targeted-therapies,[19,20] all of which help to enhance clinical awareness to this disease. Recent studies reported an increased prevalence of CA in the population of patients with HF and preserved ejection fraction,[21] which is also characterized by increased wall thickening and LV diastolic impairment. Indeed, the echocardiographic phenotype of CA patients, as evident by our findings and others,[2-4] is characterized by increased wall thickness and LV mass, biatrial enlargement, high E/A ratio and a high E/e' ratio reflecting high LV filling pressures. As previously reported,[3,22] we found that patients with ATTR versus AL CA were more likely to display a higher degree of structural and functional impairment as manifested by increased wall thickness, higher LV mass and worse LV systolic dysfunction; differences that were evident along the course of disease progression. ATTR is clinically characterized by fewer systemic manifestations and require patient's referral to a specific imaging study (99mTC-PYP scan), possibly accounting for its relatively late diagnosis and worse echocardiographic features compared with AL. Nevertheless, the echocardiographic findings concomitant with the diagnosis of amyloidosis, regardless of its pathogenetic subtype, reflect in the majority of cases an already advanced cardiomyopathy and portend poor prognosis.[2,23,24]

The paucity of data regarding the echocardiographic evolution of CA is surprising. To the best of our knowledge, this is the first study that describes the echocardiographic features and natural history of AL and ATTR CA in the early stages of disease, before diagnosis and initiation of targeted therapy. We found that increased wall thickness, most probably reflecting intra-myocardial amyloid infiltration, was the first echocardiographic expression of CA and appeared approximately ≥ 3 years before disease diagnosis. Moreover, RWT, a measure of LV concentric hypertrophy, was found to be abnormal ≥ 7 year preamyloid diagnosis. These early echocardiographic findings were recently shown to be associated with a high diagnostic accuracy for CA, both in the populations of patients with AL and in patients with concentric hypertrophy.[16] Notably, significantly increased wall thickness mimicking true LV hypertrophy was evident in patients who were yet undiagnosed with amyloidosis; hence, highlighting CA as a significant component in the differential diagnosis of hypertrophic hearts.[25-27]

Increased wall thickness and stiffness result in diastolic impairment which was initially reported ≥ 3 years before the diagnosis of CA, and significant LV diastolic dysfunction became prevalent approximately 1≤ year <3 preamyloid diagnosis. In a survey of >500 AL patients (37% of whom had CA) the average time from initial symptoms to diagnosis was 2 years,[28] possibly reflecting the clinical manifestations of these findings.

LV systolic dysfunction, as assessed by LVEF, was preserved in the majority of CA patients until relatively late stages of disease. Nevertheless, it is important to note that cardiac output is invariably low in CA patients due to decreased ventricular volume,[29,30] and that LV impairment may be detected at earlier disease stages by using myocardial deformation imaging techniques.[3] RV dysfunction was observed concomitantly with CA diagnosis, and may have led to disease diagnosis due to the display of HF symptoms.

The early initiation of amyloid-targeted therapy in both AL and ATTR is crucial for patient's quality of life and survival.[19,23,29] We believe that data presented in this study, which describe the natural progression of cardiac amyloid involvement and its early, prediagnosis echocardiographic phenotype, will promote early disease recognition and aid clinicians in promoting this important goal.

This study has several limitations. First, our study is limited by its relatively small sample size. Moreover, the rate of patients with mutant ATTR versus wild-type ATTR in

Table 3
Echocardiographic findings and troponin levels in patients with cardiac amyloidosis at different time intervals before the diagnosis of amyloidosis stratified by the pathogenetic subtype

Variable	<1 year prediagnosis		1≤ year <3 prediagnosis		p value^	p value^^
	Amyloid transthyretin (n = 33)	Immunoglobulin light chain amyloidosis (n = 42)	Amyloid transthyretin (n = 22)	Immunoglobulin light chain amyloidosis (n = 11)		
Left ventricular ejection fraction (median)	50 (44, 58)	60 (53, 60)	60 (45, 60)	60 (60, 60)	0.009	0.098
Left ventricular ejection fraction ≤ 50%	18 (55%)	10 (24%)	7 (32%)	0 (0%)	0.008	0.026
Right ventricular dysfunction	9 (27%)	20 (48%)	1 (5%)	0 (0%)	0.080	1.000
TAPSE	15 (13, 17)	15 (13, 18)	Non-available	Non-available	0.628	
Posterior wall (cm)	1.5 (1.4, 1.8)	1.3 (1.2, 1.5)	1.3 (1.2, 1.5)	1.1 (0.9, 1.3)	<0.001	0.005
Ventricular septum (cm)	1.6 (1.5, 1.9)	1.4 (1.3, 1.6)	1.4 (1.3, 1.6)	1.2 (0.9, 1.4)	<0.001	0.030
Left ventricular end diastolic diameter (cm)	4.3 (3.7, 4.6)	4.2 (4.0, 4.5)	4.5 (4.0, 4.8)	4.6 (4.3, 4.9)	0.928	0.562
Left ventricular end systolic diameter (cm)	3.05 (2.5, 3.5)	2.8 (2.5, 3.1)	2.8 (2.5, 3.5)	2.8 (2.7, 3.0)	0.218	0.817
Relative wall thickness	0.74 (0.62, 0.92)	0.62 (0.54, 0.76)	0.58 (0.71)	0.45 (0.48)	0.004	0.004
Left atrial area (cm^2)	26 (22, 31)	24 (21, 27)	23 (18, 29)	21 (20, 27)	0.150	0.967
Left atrial diameter (cm)	4.4 (4, 4.9)	4.2 (3.7, 4.6)	4.1 (4, 4.8)	3.7 (3.3, 4.6)	0.045	0.144
Left ventricular mass index (g/m^2)	144 (129, 191)	115 (105, 146)	Non-available	Non-available	0.020	
E/A	2.4 (1.5, 3.3)	2.1 (1.6, 2.7)	Non-available	Non-available	0.610	
Diastolic grade					0.243	0.011
Normal	1(5%)	0 (0%)	0 (0%)	2 (29%)		
1	3 (14%)	1 (3%)	4 (21%)	4 (57%)		
2	7 (32%)	13 (37%)	10 (53%)	1 (14%)		
3	11 (50%)	21 (60%)	5 (26%)	0 (0%)		
Deceleration time (ms)	132 (115, 154)	157 (117, 195)	Non-available	Non-available	0.294	
e' lateral	5 (3.9, 6)	5 (4, 5)	Non-available	Non-available	0.733	
E/e' lateral	16 (13, 20)	19 (16, 23)	Non-available	Non-available	0.077	
Systolic pulmonary artery pressure (mm Hg)	42 (35, 54)	40 (30, 50)	42 (36, 58)	29 (45, 47)	0.420	0.102
Troponin (ng/L)*	68 (52, 110)	70 (48, 123)	Non-available	Non-available	0.845	0.063

Data are presented as medians (25th, 75th quartiles) or as percentages, as appropriate.
^ Statistical comparison between ATTR and AL <1 year prediagnosis.
^^ Statistical comparison between ATTR and AL 1≤ year <3 prediagnosis.
* Troponin normal laboratory range <13 ng/L.

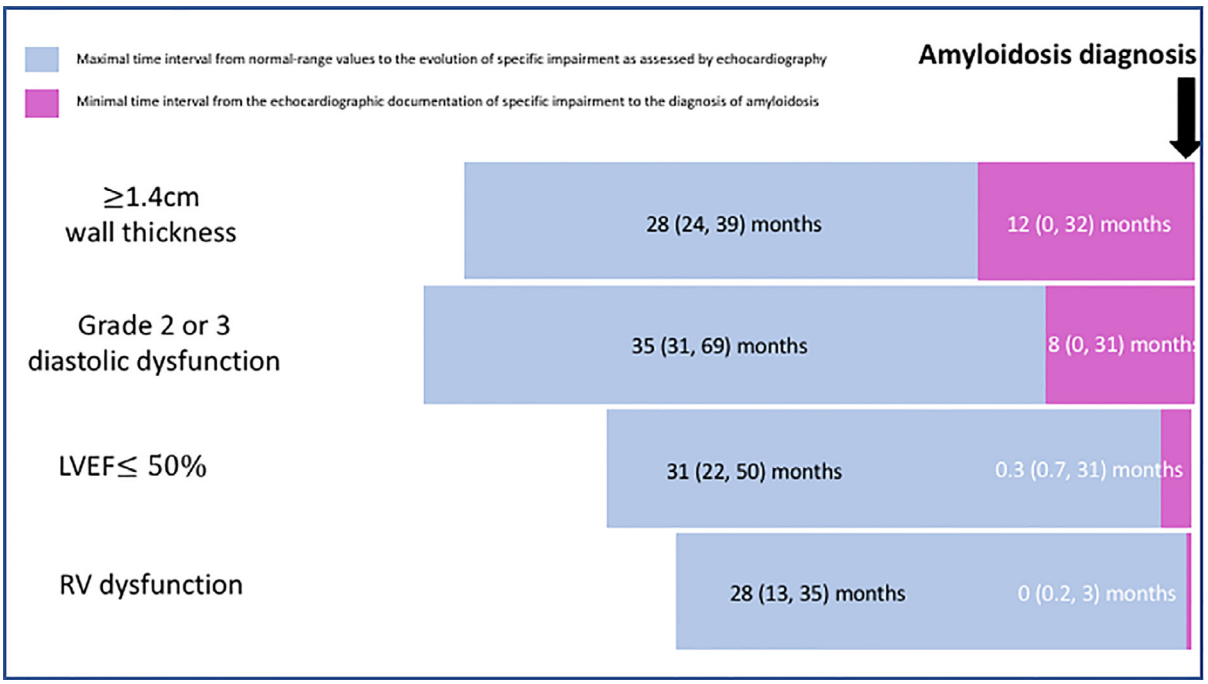

Figure 3. Time intervals in the progression of CA as assessed by echocardiography: time interval from normal to abnormal-range parameter and time interval from parameter impairment to the diagnosis of amyloidosis. Data are presented as medians (25th, 75th quartiles). CA = cardiac amyloidosis; LV = left ventricular; RV = right ventricular.

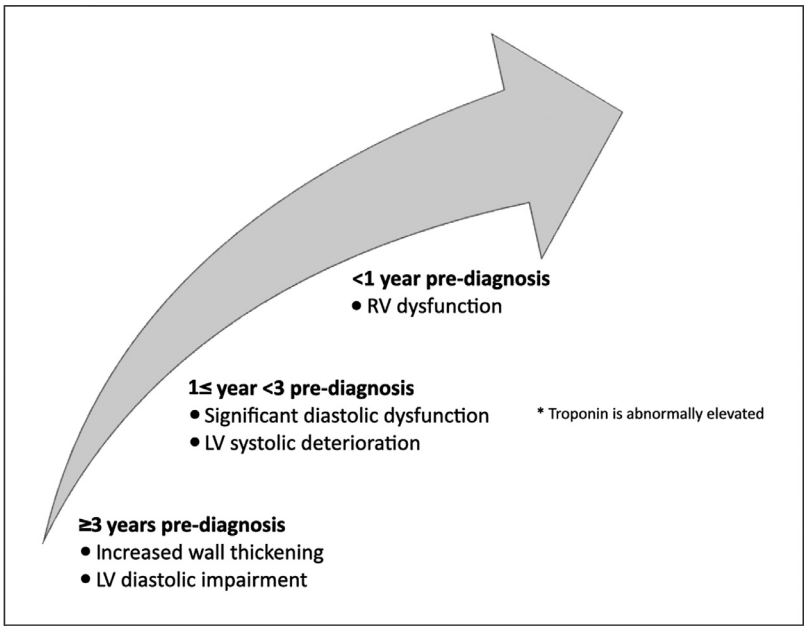

Figure 4. Schematic proposed timeline of cardiac amyloid involvement. CA = cardiac amyloidosis; LV = left ventricular; RV = right ventricular; RWT = relative wall thickness.

this cohort was low, and thus our observations may not accurately reflect the echocardiographic findings in this subpopulation. Second, since the study's observation period began more than a decade before the widespread use of cardiac scintigraphy, the diagnosis of CA in our cohort was more commonly established in patients with AL-CA compared with ATTR-CA. Third, echocardiography studies before disease diagnosis were not performed in 44% of our CA cohort, due to its retrospective nature, allowing a selection bias. Fourth, the spectrum of echocardiographic parameters used to assess cardiac amyloid involvement and diastolic dysfunction in earlier echocardiography studies was limited. This is due to the retrospective nature of this study and the fact that specific evaluation techniques, such as global longitudinal strain, were not routinely used at our institution during the study observation period. Fifth, echocardiographic findings such as increased wall thickness and diastolic dysfunction could potentially be explained by ageing. To address this limitation we defined significant wall thickness and significant diastolic dysfunction as at least moderate in severity according to published normal-range reference values.[11,15-18]

In conclusion, the structural and functional abnormalities of amyloid cardiac burden develop over a time course of several years, and may be diagnosed in their earlier stages by standard echocardiographic parameters. Early diagnosis and treatment may pave the way for improved prognosis in CA.

Disclosures

The authors have no conflicts of interest to disclose.

Authors' Contribution

Osnat Itzhaki Ben Zadok: Conceptualization, Methodology, Writing- original draft, Writing-Review and Editing; Alon Eisen: Methodology, Writing-Review and Editing; Yaron Shapira: Writing-Review and Editing; Daniel Monakier: Writing-Review and Editing; Zaza Iakobishvili: Writing-Review and Editing; Shmuel Schwartzenberg: Writing-Review and Editing; Aryeh Abelow: Writing-Review and Editing; Hadass Ofek: Writing-Review and Editing; Shirit Kazum: Writing-Review and Editing; Binyamin Ben-Avraham: Writing-Review and Editing; Ashraf Hamdan: Writing-Review and Editing; Tamir Bental: Data curation; Alik Sagie: Writing-Review and Editing; Ran Kornowski: Writing-Review and Editing, Supervision; and Mordehay Vaturi: Methodology, Supervision, Writing-Review, and Editing.

Supplementary materials

Supplementary material associated with this article can be found in the online version at https://doi.org/10.1016/j.amjcard.2020.07.050.

1. Maurer MS, Elliott P, Comenzo R, Semigran M, Rapezzi C. Addressing common questions encountered in the diagnosis and management of cardiac amyloidosis. *Circulation* 2017;135:1357–1377.
2. Dorbala S, Cuddy S, Falk RH. How to image cardiac amyloidosis: a practical approach. *JACC Cardiovasc Imaging* 2019:1368–1383.
3. Quarta CC, Solomon SD, Uraizee I, Kruger J, Longhi S, Ferlito M, Gagliardi C, Milandri A, Rapezzi C, Falk RH. Left ventricular structure and function in transthyretin-related versus light-chain cardiac amyloidosis. *Circulation* 2014;129:1840–1849.
4. Chacko L, Martone R, Bandera F, Lane T, Martinez-Naharro A, Boldrini M, Rezk T, Whelan C, Quarta C, Rowczenio D, Gilbertson JA, Wongwarawipat T, Lachmann H, Wechalekar A, Sachchithanantham S, Mahmood S, Marcucci R, Knight D, Hutt D, Moon J, Petrie A, Cappelli F, Guazzi M, Hawkins PN, Gillmore JD, Fontana M. Echocardiographic phenotype and prognosis in transthyretin cardiac amyloidosis. *Eur Heart J* 2020;41:1439–1447.
5. Falk RH, Quarta CC. Echocardiography in cardiac amyloidosis. *Heart Fail Rev* 2015;20:125–131.

6. Dorbala S, Ando Y, Bokhari S, Dispenzieri A, Falk RH, Ferrari VA, Fontana M, Gheysens O, Gillmore JD, Glaudemans A, Hanna MA, Hazenberg BPC, Kristen AV, Kwong RY, Maurer MS, Merlini G, Miller EJ, Moon JC, Murthy VL, Quarta CC, Rapezzi C, Ruberg FL, Shah SJ, Slart R, Verberne HJ, Bourque JM. ASNC/AHA/ASE/EANM/HFSA/ISA/SCMR/SNMMI expert consensus recommendations for multimodality imaging in cardiac amyloidosis: part 1 of 2-evidence base and standardized methods of imaging. *J Card Fail* 2019;25:e1–e39.
7. Itzhaki Ben Zadok O, Abelow A, Vaxman I, Eisen A, Iakobishvili Z, Sagie A, Kornowski R, Vaturi M. Prior carpal tunnel syndrome and early concomitant echocardiographic findings among patients with cardiac amyloidosis. *J Card Fail* 2020;S1071-9164(20)30197-4. https://doi.org/10.1016/j.cardfail.2020.06.009. Online ahead of print.
8. Merlini G, Dispenzieri A, Sanchorawala V, Schonland SO, Palladini G, Hawkins PN, Gertz MA. Systemic immunoglobulin light chain amyloidosis. *Nat Rev Dis Primers* 2018;4:38.
9. Perugini E, Guidalotti PL, Salvi F, Cooke RM, Pettinato C, Riva L, Leone O, Farsad M, Ciliberti P, Bacchi-Reggiani L, Fallani F, Branzi A, Rapezzi C. Noninvasive etiologic diagnosis of cardiac amyloidosis using 99mTc-3,3-diphosphono-1,2-propanodicarboxylic acid scintigraphy. *J Am Coll Cardiol* 2005;46:1076–1084.
10. Gillmore JD, Maurer MS, Falk RH, Merlini G, Damy T, Dispenzieri A, Wechalekar AD, Berk JL, Quarta CC, Grogan M, Lachmann HJ, Bokhari S, Castano A, Dorbala S, Johnson GB, Glaudemans AW, Rezk T, Fontana M, Palladini G, Milani P, Guidalotti PL, Flatman K, Lane T, Vonberg FW, Whelan CJ, Moon JC, Ruberg FL, Miller EJ, Hutt DF, Hazenberg BP, Rapezzi C, Hawkins PN. Nonbiopsy diagnosis of cardiac transthyretin amyloidosis. *Circulation* 2016;133:2404–2412.
11. Lang RM, Badano LP, Mor-Avi V, Afilalo J, Armstrong A, Ernande L, Flachskampf FA, Foster E, Goldstein SA, Kuznetsova T, Lancellotti P, Muraru D, Picard MH, Rietzschel ER, Rudski L, Spencer KT, Tsang W, Voigt JU. Recommendations for cardiac chamber quantification by echocardiography in adults: an update from the American Society of Echocardiography and the European Association of Cardiovascular Imaging. *J Am Soc Echocardiogr* 2015;28:1–39. e14.
12. Devereux RB, Reichek N. Echocardiographic determination of left ventricular mass in man. Anatomic validation of the method. *Circulation* 1977;55:613–618.
13. Rudski LG, Lai WW, Afilalo J, Hua L, Handschumacher MD, Chandrasekaran K, Solomon SD, Louie EK, Schiller NB. Guidelines for the echocardiographic assessment of the right heart in adults: a report from the American Society of Echocardiography endorsed by the European Association of Echocardiography, a registered branch of the European Society of Cardiology, and the Canadian Society of Echocardiography. *J Am Soc Echocardiogr* 2010;23:685–713. quiz 786-688.
14. Silbiger JJ. Pathophysiology and echocardiographic diagnosis of left ventricular diastolic dysfunction. *J Am Soc Echocardiogr* 2019;32:216–232. e212.
15. Nagueh SF, Smiseth OA, Appleton CP, Byrd BF 3rd, Dokainish H, Edvardsen T, Flachskampf FA, Gillebert TC, Klein AL, Lancellotti P, Marino P, Oh JK, Alexandru Popescu B, Waggoner AD. Recommendations for the evaluation of left ventricular diastolic function by echocardiography: an update from the American Society of Echocardiography and the European Association of Cardiovascular Imaging. *Eur Heart J Cardiovasc Imaging* 2016;17:1321–1360.
16. Boldrini M, Cappelli F, Chacko L, Restrepo-Cordoba MA, Lopez-Sainz A, Giannoni A, Aimo A, Baggiano A, Martinez-Naharro A, Whelan C, Quarta C, Passino C, Castiglione V, Chubuchnyi V, Spini V, Taddei C, Vergaro G, Petrie A, Ruiz-Guerrero L, Monivas V, Mingo-Santos S, Mirelis JG, Dominguez F, Gonzalez-Lopez E, Perlini S, Pontone G, Gillmore J, Hawkins PN, Garcia-Pavia P, Emdin M, Fontana M. Multiparametric echocardiography scores for the diagnosis of cardiac amyloidosis. *JACC Cardiovasc Imaging* 2019:909–920.
17. Kou S, Caballero L, Dulgheru R, Voilliot D, De Sousa C, Kacharava G, Athanassopoulos GD, Barone D, Baroni M, Cardim N, Gomez De Diego JJ, Hagendorff A, Henri C, Hristova K, Lopez T, Magne J, De La Morena G, Popescu BA, Penicka M, Ozyigit T, Rodrigo Carbonero JD, Salustri A, Van De Veire N, Von Bardeleben RS, Vinereanu D, Voigt JU, Zamorano JL, Donal E, Lang RM, Badano LP, Lancellotti P. Echocardiographic reference ranges for normal cardiac chamber size: results from the NORRE study. *Eur Heart J Cardiovasc Imaging* 2014;15:680–690.
18. Caballero L, Kou S, Dulgheru R, Gonjilashvili N, Athanassopoulos GD, Barone D, Baroni M, Cardim N, Gomez de Diego JJ, Oliva MJ, Hagendorff A, Hristova K, Lopez T, Magne J, Martinez C, de la Morena G, Popescu BA, Penicka M, Ozyigit T, Rodrigo Carbonero JD, Salustri A, Van De Veire N, Von Bardeleben RS, Vinereanu D, Voigt JU, Zamorano JL, Bernard A, Donal E, Lang RM, Badano LP, Lancellotti P. Echocardiographic reference ranges for normal cardiac Doppler data: results from the NORRE Study. *Eur Heart J Cardiovasc Imaging* 2015;16:1031–1041.
19. Maurer MS, Schwartz JH, Gundapaneni B, Elliott PM, Merlini G, Waddington-Cruz M, Kristen AV, Grogan M, Witteles R, Damy T, Drachman BM, Shah SJ, Hanna M, Judge DP, Barsdorf AI, Huber P, Patterson TA, Riley S, Schumacher J, Stewart M, Sultan MB, Rapezzi C. Tafamidis treatment for patients with transthyretin amyloid cardiomyopathy. *NEJM* 2018;379:1007–1016.
20. Gertz MA. Immunoglobulin light chain amyloidosis: 2018 update on diagnosis, prognosis, and treatment. *Am J Hematol* 2018;93:1169–1180.
21. Gonzalez-Lopez E, Gallego-Delgado M, Guzzo-Merello G, de Haro-Del Moral FJ, Cobo-Marcos M, Robles C, Bornstein B, Salas C, Lara-Pezzi E, Alonso-Pulpon L, Garcia-Pavia P. Wild-type transthyretin amyloidosis as a cause of heart failure with preserved ejection fraction. *Eur Heart J* 2015;36:2585–2594.
22. Sperry BW, Vranian MN, Hachamovitch R, Joshi H, McCarthy M, Ikram A, Hanna M. Are classic predictors of voltage valid in cardiac amyloidosis? A contemporary analysis of electrocardiographic findings. *Int J Cardiol* 2016;214:477–481.
23. Witteles RM, Liedtke M. AL amyloidosis for the cardiologist and oncologist. *Epidemiol Diagn Manage* 2019;1:117–130.
24. Ruberg FL, Grogan M, Hanna M, Kelly JW, Maurer MS. Transthyretin amyloid cardiomyopathy: JACC state-of-the-art review. *J Am Coll Cardiol* 2019;73:2872–2891.
25. Elliott PM, Anastasakis A, Borger MA, Borggrefe M, Cecchi F, Charron P, Hagege AA, Lafont A, Limongelli G, Mahrholdt H, McKenna WJ, Mogensen J, Nihoyannopoulos P, Nistri S, Pieper PG, Pieske B, Rapezzi C, Rutten FH, Tillmanns C, Watkins H. 2014 ESC guidelines on diagnosis and management of hypertrophic cardiomyopathy: the Task Force for the Diagnosis and Management of Hypertrophic Cardiomyopathy of the European Society of Cardiology (ESC). *Eur Heart J* 2014;35:2733–2779.
26. Vermeer AMC, Janssen A, Boorsma PC, Mannens M, Wilde AAM, Christiaans I. Transthyretin amyloidosis: a phenocopy of hypertrophic cardiomyopathy. *Amyloid* 2017;24:87–91.
27. Sattar Y, Ruiz Maya T, Zafrullah F, Patel NB, Latchana S. Diagnosis and management of a cardiac amyloidosis case mimicking hypertrophic cardiomyopathy. *Cureus* 2018;10:e3749.
28. Lousada I, Comenzo RL, Landau H, Guthrie S, Merlini G. Light chain amyloidosis: patient experience survey from the amyloidosis research consortium. *Adv Ther* 2015;32:920–928.
29. Falk RH, Alexander KM, Liao R, Dorbala S. AL (light-chain) cardiac amyloidosis: a review of diagnosis and therapy. *J Am Coll Cardiol* 2016;68:1323–1341.
30. Donnelly JP, Hanna M. Cardiac amyloidosis: an update on diagnosis and treatment. *Cleve Clin J Med* 2017;84:12–26.